J|A|C|S
ARTICLES

Published on Web 03/01/2010

Self-Assembly of Linear−Dendritic Diblock Copolymers: From Nanofibers to Polymersomes

Jesús del Barrio,† Luis Oriol,*,† Carlos Sánchez,*,‡ José Luis Serrano,§ Aurélie Di Cicco,‖ Patrick Keller,‖ and Min-Hui Li*,‖,⊥

Departamento de Química Orgánica y Química Física, Facultad de Ciencias-Instituto de Ciencia de Materiales de Aragón, Universidad de Zaragoza-CSIC, 50009 Zaragoza, Spain, Departamento de Física de la Materia Condensada, Facultad de Ciencias-Instituto de Ciencia de Materiales de Aragón, Universidad de Zaragoza-CSIC, 50009 Zaragoza, Spain, Instituto Universitario de Nanociencia de Aragón, Universidad de Zaragoza, 50009 Zaragoza, Spain, Institut Curie, CNRS, Université Pierre et Marie Curie, UMR168, Laboratoire Physico-Chimie Curie, 26 rue d'Ulm, 75248 Paris Cedex 05, France, and Key Laboratory of Molecular Engineering of Polymers, Fudan University, Shanghai 200433, China

Received October 2, 2009; E-mail: loriol@unizar.es; carloss@unizar.es; min-hui.li@curie.fr

Abstract: We report the formation of cylindrical micelles, sheet-like micelles, tubular micelles, as well as polymer vesicles by a new series of amphiphilic linear−dendritic block-copolymers (BCs). The BCs, noted as **PEG*m*-AZO*n***, are composed of poly(ethylene glycol) (PEG) chains of different molecular weights as hydrophilic blocks and the first four generations of azobenzene-containing dendrons based on 2,2-bis(hydroxymethyl)propionic acid (bis-MPA) as hydrophobic blocks (*m* represents the degree of polymerization of PEG, and *n* is the number of azobenzene units at the periphery of dendron). The polymeric aggregates were formed by adding water to solutions of the BCs in dioxane. The micellar dispersions in water were finally obtained by removing dioxane via dialysis against water. The morphology of the micellar self-assemblies was studied by transmission electron microscopy (TEM), cryo-electron microscopy (cryo-TEM), and atomic force microscopy (AFM). A generation-dependent aggregation behavior was found for the series of BCs **PEG45-AZO*n***. Core−shell structured nanofibers with an inner diameter of 8 nm were observed for the copolymer **PEG45-AZO2** (hydrophilic/hydrophobic weight ratio equal to 67/33). Lyotropic liquid crystalline behavior was detected for the aqueous solution of the nanofibers. The coexistence of sheet-like aggregates and tubular micelles was detected for the copolymer **PEG45-AZO8** in which the number of cyanoazobenzene units is increased to 8 (hydrophilic/hydrophobic weight ratio equal to 33/67). The tubular micelles could be intermediates in the sheet-like aggregate-to-vesicle transition. Polymer vesicles (polymersomes) with a diameter in the range 300−800 nm were observed for the copolymer **PEG45-AZO16** (hydrophilic/hydrophobic weight ratio equal to 20/80). The membrane of the sheet-like aggregates, tubular micelles, and polymersomes was shown to have a bilayer structure, as revealed by cryo-TEM. UV illumination of the aqueous polymersome dispersion induced the formation of wrinkles in the vesicle membrane, thus showing that this type of polymeric aggregate is photoresponsive.

Introduction

The sustained interest in micellar aggregates obtained from amphiphilic block copolymers (BCs) arises from their potential numerous applications such as drug delivery systems,[1−4] nanoreactors,[5−8] and nanotemplates.[9] When compared to micelles from traditional surfactants, polymeric self-assemblies have recently been recognized for advantages such as superior stability, toughness, micellization depending on selective solvents, and the ability to trap metastable structures due to slow kinetics.[10−13] Moreover, polymeric self-assemblies offer numerous possibilities to tailor physical, chemical, and biological properties by variation of the block copolymer chemical structure or by conjugation of biomolecules.[14] In many instances, the morphology of the polymeric self-assembly and its application are closely related. Thus, controlling the morphology of

---

[†] Departamento de Química Orgánica y Química Física, ICMA; Universidad de Zaragoza-CSIC.

[‡] Departamento de Física de la Materia Condensada, ICMA; Universidad de Zaragoza-CSIC.

[§] Instituto Universitario de Nanociencia de Aragón, Universidad de Zaragoza.

[‖] Institut Curie and CNRS.

[⊥] Fudan University.

(1) Savic, R.; Luo, L.; Eisenberg, A.; Maysinger, D. *Science* **2003**, *300*, 615.
(2) Discher, D. E.; Ortiz, V.; Srinivas, G.; Klein, M. L.; Kim, Y.; Christian, D.; Cai, S.; Photos, P.; Ahmed, F. *Prog. Polym. Sci.* **2007**, *32*, 838.
(3) Gilles, E. R.; Frechet, J. M. J. *J. Am. Chem. Soc.* **2002**, *124*, 14137.
(4) Gilles, E. R.; Dy, E.; Frechet, J. M. J.; Szoka, F. C. *Mol. Pharmacol.* **2005**, *2*, 129.
(5) Chan, Y. N. C.; Schrock, R. R.; Cohen, R. E. *Chem. Mater.* **1992**, *4*, 24.
(6) Vriezema, D. M.; Hoogboom, J.; Velonia, K.; Takazawa, K.; Christianen, P. C. M.; Maan, J. C.; Rowan, A. E.; Nolte, R. J. M. *Angew. Chem.* **2003**, *115*, 796.

10.1021/ja9083946

the assembled structures from BCs is of great practical value. Polymer micelle morphology and size can be designed through the adequate selection of the nature and length of the different blocks, the use of controlled electrostatic interactions between polymeric chains, or the modification of the macromolecular architecture.[15−28] A great deal of the experimental research has been directed toward the study of the self-assembly of linear coil−coil and rod−coil BCs. However, the introduction of a dendritic structure as a building block in the design of novel BCs provides some interesting opportunities.[29−36] Dendritic moieties have a well-defined branched architecture and a highly organized inner part.[37−39] Moreover, these systems can be made amphiphilic through appropriate functionalization of their focal point and peripheral groups.[40,41] The combination of linear hydrophilic and dendritic hydrophobic blocks,[37,42−54] or of linear hydrophobic and dendritic hydrophilic blocks,[55−68] has proven to be an interesting approach to build amphiphilic block copolymers that can give rise to supramolecular aggregates in solution. Most studies deal with the formation of spherical micelles from linear−dendritic BCs, while there are only a few papers concerning other morphologies such as cylindrical micelles or polymer vesicles (polymersomes) tailored by the length of the blocks.[55−58,63−68] On the other hand, many potential applications require supramolecular aggregates that can be destabilized by external stimuli, for example, to control the release of encapsulated substances. Nevertheless, there are only a few reports on stimuli-responsive amphiphilic linear−dendritic BCs, and these are limited to pH-,[44,55] solvent-,[66] and thermal-sensitive[37] systems.

Azobenzene molecules undergo isomerization between the trans and cis states when they are irradiated in their absorption bands. The polarity, shape, and size changes that azobenzene undergoes after isomerization modify significantly the structures and properties of azobenzene-containing polymer blocks. The synthesis and self-assembly behavior of amphiphilic linear BCs bearing azobenzene groups have already attracted widespread attention.[69−83] Light-responsive azopolymer micelles and vesicles with rather different triggering mechanisms have been repor-

---

(7) Gitsov, I.; Hamzik, J.; Ryan, J.; Simonyan, A.; Nakas, J. P.; Omori, Sh.; Krastanov, A.; Cohen, T.; Tanenbaum, S. W. *Biomacromolecules* **2008**, *9*, 804.

(8) Simonyan, A.; Gitsov, I. *Langmuir* **2008**, *24*, 11431.

(9) Hamley, I. W. *Angew. Chem., Int. Ed.* **2003**, *42*, 1692.

(10) Cui, H.; Chen, Z.; Wooley, K. L.; Pochan, D. J. *Macromolecules* **2006**, *39*, 6599.

(11) Lodge, T. P. *Macromol. Chem. Phys.* **2003**, *204*, 265.

(12) Discher, B. M.; Won, Y. Y.; Ede, D. S.; Lee, J. C. M.; Bates, F. S.; Discher, D. E.; Hammer, D. A. *Science* **1999**, *284*, 1143.

(13) Riess, G. *Prog. Polym. Sci.* **2003**, *28*, 1107.

(14) Dirks, A. J. T.; van Berkel, S. S.; Hatzakis, N. S.; Opsteen, J. A.; van Delft, F. L.; Cornelissen, J. J. L. M.; Rowan, A. E.; van Hest, J. C. M.; Rutjes, F. P. J. T.; Nolte, R. J. M. *Chem. Commun.* **2005**, *33*, 4172.

(15) Hadjichristidis, N.; Pispas, S.; Floudas, G. A. *Block Copolymers*; Wiley Interscience: New York, 2003.

(16) Ott, C.; Hoogenboom, R.; Hoeppener, S.; Wouters, D.; Gohy, J.-F.; Schubert, U. S. *Soft Matter* **2009**, *5*, 84.

(17) Pochan, D. J.; Chen, Z.; Cui, H.; Hales, K.; Qi, K.; Wooley, K. L. *Science* **2004**, *306*, 94.

(18) Chen, Z.; Cui, H.; Hales, K.; Li, Z.; Qi, K.; Pochan, D. J.; Wooley, K. L. *J. Am. Chem. Soc.* **2005**, *127*, 8592.

(19) Li, Z.; Kesselman, E.; Talmon, Y.; Hillmyer, M. A.; Lodge, T. P. *Science* **2004**, *306*, 98.

(20) Jain, S.; Bates, F. *Science* **2003**, *300*, 460.

(21) Zhang, L.; Eisenberg, A. *Science* **1995**, *268*, 1728.

(22) Yan, X.; Liu, G.; Zhao, L. *J. Am. Chem. Soc.* **2004**, *126*, 10059.

(23) *Block Copolymers in Nanoscience*; Lazzari, M., Liu, G. J., Lecommandoux, S., Eds.; Wiley-VCH: Weinheim, 2006.

(24) Hoogenboom, R.; Wiesbrock, F.; Leenen, M. A. M.; Thijs, H. M. L.; Huang, T.; Fustin, C.-H.; Guillet, P.; Gohy, J.-F.; Schubert, U. S. *Macromolecules* **2007**, *40*, 2837.

(25) Zhang, J.; Yu, K.; Eisenberg, A. *Science* **1996**, *272*, 1777.

(26) Geng, Y.; Ahmed, F.; Bhasin, N.; Discher, D. E. *J. Phys. Chem. B* **2005**, *109*, 3772.

(27) Cui, H.; Chen, Z.; Zhong, S.; Wooley, K. L.; Pochan, D. J. *Science* **2007**, *317*, 647.

(28) Christian, D. A.; Tian, A.; Ellenbroek, W. G.; Levental, I.; Rajagopal, K.; Janmey, P. A.; Liu, A. J.; Baumgart, T.; Discher, D. E. *Nat. Mater.* **2009**, *8*, 843.

(29) Hawker, C. J.; Wooley, K. L. *Science* **2005**, *309*, 1200.

(30) Pyun, J.; Zhou, X.; Drockenmuller, E.; Hawker, C. J. *J. Mater. Chem.* **2003**, *13*, 2653.

(31) Lee, C. C.; Mackay, J. A.; Frechet, J. M. J.; Szoka, F. C. *Nat. Biotechnol.* **2005**, *23*, 1517.

(32) Gitsov, I.; Frechet, J. M. J. *Macromolecules* **1994**, *27*, 7309.

(33) Leduc, M. R.; Hawker, C. J.; Dao, J.; Frechet, J. M. J. *J. Am. Chem. Soc.* **1996**, *118*, 11111.

(34) Gilles, E. R.; Jonsson, T. B.; Frechet, J. M. J. *J. Am. Chem. Soc.* **2004**, *126*, 11936.

(35) Frechet, J. M. J. *Science* **1994**, *263*, 1710.

(36) Gitsov, I. *J. Polym. Sci., Part A: Polym. Chem.* **2008**, *46*, 5295.

(37) Ge, Z.; Luo, S.; Liu, S. *J. Polym. Sci., Part A: Polym. Chem.* **2006**, *44*, 1357.

(38) Bosman, A. W.; Janssen, H. M.; Meijer, E. W. *Chem. Rev.* **1999**, *99*, 1665.

(39) Tomalia, D. A. *Prog. Polym. Sci.* **2005**, *30*, 294.

(40) Hecht, S. *J. Polym. Sci., Part A: Polym. Chem.* **2003**, *41*, 1047.

(41) Gitsov, I.; Lin, C. *Curr. Org. Chem.* **2005**, *9*, 1025.

(42) Gitsov, I.; Wooley, K. L.; Fréchet, J. M. J. *Angew. Chem., Int. Ed. Engl.* **1992**, *31*, 1200.

(43) Gitsov, I.; Fréchet, J. M. J. *Macromolecules* **1993**, *26*, 6536.

(44) Gillies, E. R.; Jonsson, T. B.; Fréchet, J. M. J. *J. Am. Chem. Soc.* **2004**, *126*, 11936.

(45) Chapman, T. M.; Hillyer, G. L.; Mahan, E. J.; Shaffer, K. A. *J. Am. Chem. Soc.* **1994**, *116*, 11195.

(46) Gitsov, I.; Lambrych, K. R.; Remnant, V. A.; Pracitto, R. *J. Polym. Chem., Part A: Polym. Chem.* **2000**, *28*, 2711.

(47) Chang, Y.; Park, C.; Kim, K. T.; Kim, C. *Langmuir* **2005**, *21*, 4334.

(48) Chang, Y.; Kwon, Y. C.; Lee, S. C.; Kim, C. *Macromolecules* **2000**, *33*, 4496.

(49) Chang, Y. Y.; Kim, C. *J. Polym. Chem., Part A: Polym. Chem.* **2001**, *39*, 918.

(50) Hua, C.; Peng, S. M.; Dong, C. M. *Macromolecules* **2008**, *41*, 6686.

(51) Peng, S. M.; Chen, Y.; Hua, C.; Dong, C. M. *Macromolecules* **2009**, *42*, 104.

(52) Namazi, H.; Adeli, M. *J. Polym. Chem., Part A: Polym. Chem.* **2005**, *43*, 28.

(53) Fernández-Megía, E.; Correa, J.; Riguera, R. *Biomacromolecules* **2006**, *7*, 3104.

(54) Gitsov, I.; Simonyan, A.; Vladimirov, N. G. *J. Polym. Chem., Part A: Polym. Chem.* **2007**, *45*, 5136.

(55) van Hest, J. C. M.; Baars, M. W. P. L.; Elissen- Román, C.; van Genderen, M. H. P.; Meijer, E. W. *Macromolecules* **1995**, *28*, 6689.

(56) van Hest, J. C. M.; Delnoye, D. A. P.; Baars, M. W. P. L.; van Genderen, M. H. P.; Meijer, E. W. *Science* **1995**, *268*, 1592.

(57) Tian, L.; Nguyen, P.; Hammond, P. T. *Chem. Commun.* **2006**, *33*, 3489.

(58) Tian, L.; Hammond, P. T. *Chem. Mater.* **2006**, *18*, 3976.

(59) Nguyen, P. M.; Zacharia, N. S.; Verploegen, E.; Hammond, P. T. *Chem. Mater.* **2007**, *19*, 5524.

(60) Iyer, J.; Fleming, K.; Hammond, P. T. *Macromolecules* **1998**, *31*, 8757.

(61) Aoi, K.; Motoda, A.; Okada, M. *Macromol. Rapid Commun.* **1997**, *18*, 945.

(62) Istratov, V.; Kautz, H.; Kim, Y.-K.; Schubert, R.; Frey, H. *Tetrahedron* **2003**, *59*, 4017.

(63) Jang, C.-J.; Ryu, J.-H.; Lee, J.-D.; Sohn, D.; Lee, M. *Chem. Mater.* **2004**, *16*, 4226.

(64) Yoo, Y.-S.; Choi, J.-H.; Song, J.-H.; Oh, N.-K.; Zin, W.-C.; Park, S.; Chang, T.; Lee, M. *J. Am. Chem. Soc.* **2004**, *126*, 6294.

(65) Holzmueller, J.; Genson, K. L.; Park, Y.; Yoo, Y.-S.; Park, M.-H.; Lee, M.; Tsukruk, V. *Langmuir* **2005**, *21*, 6392.

(66) Kim, J.-K.; Lee, E.; Lee, M. *Angew. Chem., Int. Ed.* **2006**, *45*, 7195.

(67) Zubarev, E. R.; Sone, E. D.; Stupp, S. I. *Chem.-Eur. J.* **2006**, *12*, 7313.

(68) Gans, B. J.; Wiegand, S.; Zubarev, E. R.; Stupp, S. I. *J. Phys. Chem. B* **2002**, *106*, 9730.

ted.[81,83] In the reported azopolymer micelles,[81] solubilization of the hydrophobic azopolymer block in dioxane/water mixtures caused by the trans-to-cis isomerization of azobenzene (polarity change) was claimed to be responsible for micelle disruption in this dioxane/water solvent mixture. Li and co-workers[83] recently reported polymersome bursting induced by the creation of spontaneous curvature in the asymmetrical vesicles composed of a liquid crystalline (LC) rod-like azopolymer in one membrane leaflet and an inert coil polymer in other leaflet. The rod-to-coil conformational change in the LC polymer block caused by the trans-to-cis isomerization of azobenzene (shape change) is responsible for the surface area increase in the azopolymer leaflet and the creation of spontaneous curvature of the membrane. Light is an advantageous stimulus as compared to other stimuli, such as pH, solvent, or temperature changes, because it is a rapid and remote stimulus that does not require any change in the chemical environment and can be applied locally.

There is particular interest in the synthesis of azobenzene-containing BCs that have a well-defined structure. In this respect, we recently reported the synthesis and characterization of a new series of amphiphilic poly(ethylene glycol)-*b*-azodendron BCs with a hydrophilic linear poly(ethylene glycol) (PEG) block ($M_n = 2000$ and degree of polymerization, $m = 45$) and a hydrophobic block based on the first four generations of aliphatic polyester dendrons functionalized at the periphery with cyanoazobenzene mesogens.[84] The incorporation of azobenzene moieties into the BC through a dendritic block enables perfect control of the number of photochromic moieties. We describe here the aqueous self-assembly of this new type of amphiphilic linear−dendritic BCs, which are denoted as **PEG*m*-AZO*n***. The general chemical structure of these BCs is shown in Chart 1 (the individual chemical structures of each of the BCs can be found in the Supporting Information). In comparison to other types of amphiphilic linear−dendritic BCs with a hydrophobic rigid dendritic block,[32,36,42,46,54] the aliphatic dendritic matrix of **PEG*m*-AZO*n*** is flexible enough to enable the reorganization of the cyanoazobenzene mesogenic moieties during aggregation, and this is a key point in obtaining self-assemblies with different morphologies. In fact, by changing the generation number of the dendritic block ($G = 1, 2, 3$, or 4; number of azobenzene mesogens $n = 2^G$; see Chart 1) or the length of the PEG block, polymeric aggregates with different morphologies, such as cylindrical micelles (nanofibers), sheet-like aggregates, tubular micelles, or polymersomes, were obtained (see Table 1). The fact that all azobenzene groups are located at the periphery of the dendron would result in a significant size change of the dendron during trans-to-cis isomerization. Indeed, wrinkles, and even rupture, in the membrane of the polymersome were detected upon UV irradiation of the aqueous vesicle dispersion.

Chart 1. Chemical Structure of the Linear−Dendritic Block Copolymers **PEG*m*-AZO*n***

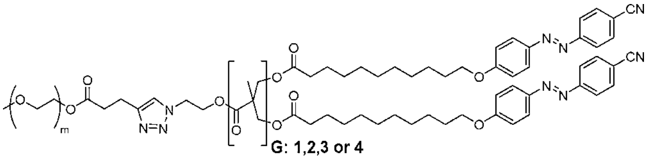

PEG*m*-AZO*n*

m: degree of polymerization (DP) of the PEG block
G: generation number of the AZO dendritic block
n: number of mesogenic units at the periphery of the AZO dendritic block ($n = 2^G$)

Results and Discussion

1. Characterization of Linear−Dendritic BCs. In a previous paper,[84] we reported the synthesis and characterization of the amphiphilic linear−dendritic BCs **PEG45-AZO*n*** ($n = 2, 4, 8, 16$), which consisted of a linear block of PEG (degree of polymerization $m = 45$) and the first four generations of aliphatic polyester dendrons functionalized at the periphery with 4-cyanoazobenzene units. For the sake of comparison, the homologous amphiphilic BCs, **PEG25-AZO16** and **PEG114-AZO16**, bearing generation 4 of the azodendron ($n = 16$) and PEG blocks with degrees of polymerization of 25 and 114, respectively, were prepared in a similar way. Characterizations by ^{1}H NMR spectroscopy, FT-IR spectroscopy, elemental analysis, and MALDI-TOF mass spectroscopy confirmed the structures of these BCs to be those presented in Chart 1. Molecular weight and composition of **PEG*m*-AZO*n*** are summarized in Table 1. Details on the synthesis and characterization of the materials are included in the Supporting Information.

The phase transitions of the BCs studied by DSC and POM upon cooling are gathered in Table 2. Birefringent textures were detected upon cooling from the isotropic state by POM for the linear−dendritic BCs having 4, 8, or 16 cyanoazobenzene mesogenic units at the periphery of the dendritic block. The isotropic-to-mesophase transition temperatures for the mesomorphic BCs were obtained from the cooling scans (see the Supporting Information). The glass transition associated with the azodendron block[84] was also detected in the cases of **PEG45-AZO8**, **PEG45-AZO16**, and **PEG25-AZO16** (the mesophase of these BCs is vitrified at temperatures around room temperature). On the other hand, **PEG45-AZO2**, **PEG45-AZO4**, and **PEG114-AZO16** crystallize upon cooling, as shown in the DSC cooling traces.

The liquid-crystalline azodendrons are not miscible with PEG blocks, and the BCs **PEG*m*-AZO*n*** can phase separate into organized bulk nanostructures. All linear−dendritic BCs exhibit lamellar-type microphase separation as confirmed by XRD and TEM studies. The lamellar phase segregation of crystalline samples of **PEG45-AZO2** and **PEG45-AZO4** and oriented glassy fibers of **PEG45-AZO8** and **PEG45-AZO16** has been

---

(69) Sin, S. L.; Gan, L. H.; Hu, X.; Tam, K. C.; Gan, Y. Y. *Macromolecules* **2005**, *38*, 3943.
(70) Ravi, P.; Sin, S. L.; Gan, L. H.; Gan, Y. Y.; Tam, K. C.; Xia, X. L.; Hu, X. *Polymer* **2005**, *46*, 137.
(71) Yang, J.; Levy, D.; Deng, W.; Keller, P.; Li, M. H. *Chem. Commun.* **2005**, *34*, 4345.
(72) Yang, J.; Piñol, R.; Gubellini, F.; Lévy, D.; Albouy, P.-A.; Keller, P.; Li, M.-H. *Langmuir* **2006**, *22*, 7907.
(73) Wang, D.; Ren, H.; Wang, X.; Wang, X. *Macromolecules* **2008**, *41*, 9382.
(74) Wang, D.; Lin, J.; Yen, G.; Wang, X. *Polymer* **2009**, *50*, 418.
(75) Su, W.; Han, K.; Luo, Y.; Wang, Z.; Li, Y.; Zhang, Q. *Macromol. Chem. Phys.* **2007**, *208*, 955.
(76) Su, W.; Luo, Y.; Yan, Q.; Wu, S.; Han, K.; Zhang, Q.; Gu, Y.; Li, Y. *Macromol. Rapid Commun.* **2007**, *28*, 1251.
(77) Li, Y.; Deng, Y.; He, Y.; Tong, X.; Wang, X. *Langmuir* **2005**, *21*, 6567.
(78) Deng, Y.; Li, Y.; Wang, X. *Macromolecules* **2006**, *39*, 6590.
(79) Tong, X.; Wang, G.; Soldera, A.; Zhao, Y. *J. Phys. Chem. B* **2005**, *109*, 20281.
(80) Bo, Q.; Zhao, Y. *Langmuir* **2007**, *23*, 5746.
(81) Wang, G.; Tong, X.; Zhao, Y. *Macromolecules* **2004**, *37*, 8911.
(82) Bo, Q.; Tong, X.; Zhao, Y.; Zhao, Y. *Macromolecules* **2009**, *41*, 3562.
(83) Mabrouk, E.; Cuvelier, D.; Brochard-Wyart, F.; Nassoy, P.; Li, M.-H. *Proc. Natl. Acad. Sci. U.S.A.* **2009**, *106*, 7294.
(84) del Barrio, J.; Oriol, L.; Sánchez, C.; Alcalá, R. *Macromolecules* **2009**, *42*, 5752.

Table 1. Molecular Composition of **PEG*m*-AZO*n*** and Polymeric Aggregate Morphology

sample name	M_n (Da) of PEG block[a]	MW (Da) of dendritic block[b]	hydrophilic/ hydrophobic wt ratio	DP of PEG block	number of azobenzene units	M_n of **PEG*m*-AZO*n***[c]	PDI of **PEG*m*-AZO*n***[c]	polymeric aggregate morphology
PEG45-AZO2	2000	982	67/33	45	2	2840	1.005	nanofibers
PEG45-AZO4	2000	1993	50/50	45	4	3870	1.002	sheet-like micelles
PEG45-AZO8	2000	4016	33/67	45	8	5930	1.001	sheet-like micelles and tubular micelles
PEG45-AZO16	2000	8061	20/80	45	16	9120	1.016	polymersomes
PEG25-AZO16	1100	8061	12/88	25	16	8720	1.011	macroscopic phase separation
PEG114-AZO16	5000	8061	38/62	114	16	12 460	1.003	sheet-like micelles

[a] Number-average molecular weight (M_n) of the commercial PEG (Sigma-Aldrich, M_n reported by the supplier) employed in the synthesis of the BCs. This M_n corresponds to the hydrophilic block. [b] Molecular weight (MW) of the hydrophobic AZO dendritic block. [c] M_n and polydispersity (PDI) of the BCs were determined by mass spectrometry.

Table 2. Transition Temperatures for **PEG*m*-AZO*n*** Linear−Dendritic Block Copolymers Detected by the Combination of DSC and POM Observations

sample	thermal transitions[a] (°C)
PEG45-AZO2	I 13 Cr_1 0 Cr_2
PEG45-AZO4	I 47 smectic 28 Cr_1 24 Cr_2
PEG45-AZO8	I 85 smectic 6 g
PEG45-AZO16	I 112 smectic 17 g
PEG25-AZO16	I 108 smectic 12 g
PEG114-AZO16	I 116 smectic 23 Cr

[a] Thermal transition determined by DSC from the peak maximum upon cooling (scan rate: −10 °C min^{-1}). The textures observed by POM for the liquid-crystalline BCs in the smectic mesophase are indicative of the lamellar microsegregation (see text).

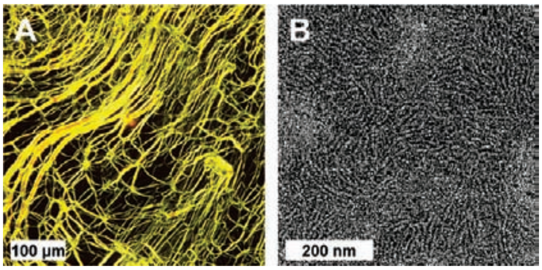

Figure 1. POM micrograph of the first cooling scan of **PEG114-AZO16** at 110 °C (A). TEM image of a thin film of **PEG114-AZO16** stained with RuO_4 (B).

described previously.[84] XRD performed on a fiber sample of **PEG25-AZO16** resulted in a diffraction pattern that was qualitatively similar to that previously obtained from a fiber sample of **PEG45-AZO16**.[84] A lamellar distance of 7.8 nm was measured for **PEG25-AZO16**. In the case of **PEG114-AZO16**, some poorly defined focal-conic and fan-shaped textures of a smectic phase are detected. Furthermore, birefringent bands are observed across a homeotropic background, which is consistent with oily streaks appearance of a SmA phase (Figure 1A). However, an obvious sharp halo was not observed in the small-angle region of X-ray patterns obtained for this BC in the mesophase (see the Supporting Information). In this case, the layer distance corresponding to the first-order diffraction peak is too large to be detected with our X-ray diffractometer. Only a diffuse halo at 0.45 nm was observed, and this is associated with the average lateral distance between mesogens. **PEG114-AZO16** crystallizes on decreasing the temperature to 23 °C, as shown by DSC and XRD. The wide-angle region of a powder diffraction pattern obtained from a sample of **PEG114-AZO16** at RT (see Experimental Section for the thermal treatment of the sample) shows three strong diffraction rings at 0.46, 0.38, and 0.32 nm. The first two rings correspond to the crystalline PEG block, and the third is tentatively assigned to the crystal structure of the dendritic block. The lamellar microsegregation of **PEG114-AZO16** was confirmed by TEM performed on a stained thin film of the BC cast onto a copper grid. A lamellar structure with darkened PEG domains was clearly observed (Figure 1B). Similar TEM observations were made for a sample of **PEG25-AZO16**. In summary, the mesomorphic BCs segregate into a lamellar-type nanostructure when they are in the liquid-crystalline state, and the aforementioned smectic-like birefringent textures are indicative of the lamellar-type microsegregation.[85] The lamellar segregation and the hybrid macromolecular architecture of **PEG*m*-AZO*n*** constrain the cyanoazobenzene units to organize into some kind of two-dimensional nematic structure in the liquid-crystalline domains in a molecular arrangement similar to that previously proposed for another type of lamella-forming rod−coil BC showing smectic mesomorphism.[86]

2. Preparation of Polymeric Micellar Aggregates and Turbidity Measurements. Polymeric micellar aggregates in water were prepared from **PEG45-AZO*n*** (*n* = 2, 4, 8, 16) and **PEG114-AZO16** by adding water progressively into dioxane solutions of the BCs.[21] These BCs possess hydrophilic/hydrophobic ratios ranging from 67/33 to 20/80. The BC **PEG25-AZO16**, with a hydrophilic/hydrophobic ratio of 12/88, showed macroscopic phase separation on addition of water. Turbidity diagrams obtained for samples of the BCs **PEG45-AZO*n*** (*n* = 2, 4, 8, 16) and **PEG114-AZO16** during the addition of water to polymer solutions in dioxane are shown in Figure 2.

Measuring the turbidity as a function of water content is often used to follow the self-assembly and the morphological transitions of BC aggregates in solution. The jumps in turbidity correspond to the formation of self-assembled aggregates. Semiquantitative indications of the aggregate sizes can be obtained from the turbidity measurements because larger structures scatter more light.[87] As can be seen in Figure 2, **PEG45-AZO2** showed three steps in turbidity before reaching a stable value. This stepwise evolution is related to morphological changes of the polymeric aggregates on the addition of water, and it will be discussed in the next section. In contrast to **PEG45-AZO2**, the BCs **PEG45-AZO16** and **PEG45-AZO8** showed a sharp turbidity onset and then reached a stable value. This fact could indicate the direct formation of the self-assemblies. **PEG45-AZO8** (hydrophilic/hydrophobic weight ratio of 33/67) shows a turbidity onset at a lower water content than that of **PEG45-AZO16**, although the latter BC has a lower hydrophilic/hydrophobic weight ratio (20/80). This feature is not well understood and might be related to the different

---

(85) Li, M.-H.; Keller, P.; Albouy, P.-A. *Macromolecules* **2003**, *36*, 2284.
(86) Ohtake, T.; Ogasawara, M.; Ito-Akita, K.; Nishina, N.; Ujiie, S.; Ohno, H.; Kato, T. *Chem. Mater.* **2000**, *12*, 782.
(87) Choucair, A.; Lavigueur, C.; Eisenberg, A. *Langmuir* **2004**, *20*, 3894.

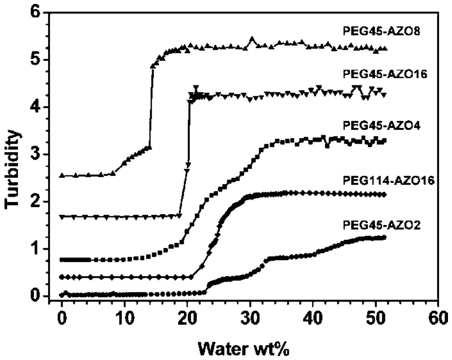

Figure 2. Turbidity curves of the linear−dendritic BC solutions in dioxane (initial concentration 1 wt %) as a function of the amount of water added to the solution. Turbidity was measured at 650 nm. The curves for the linear−dendritic BCs **PEG45-AZO*n*** ($n = 4, 8, 16$) and **PEG114-AZO16** are shifted in the vertical direction for clarity, with the turbidity being zero at a water content of 0%.

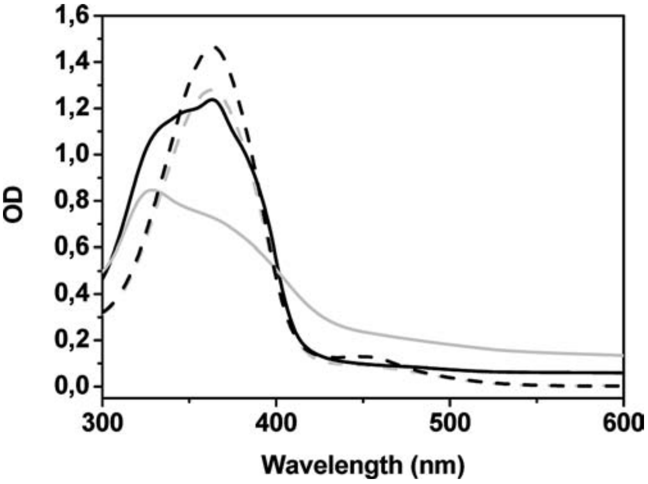

Figure 3. UV−vis spectra of the linear−dendritic BCs **PEG45-AZO2** (black lines) and **PEG45-AZO16** (gray lines) dissolved in dioxane (dashed lines) and self-assembled in water (solid lines).

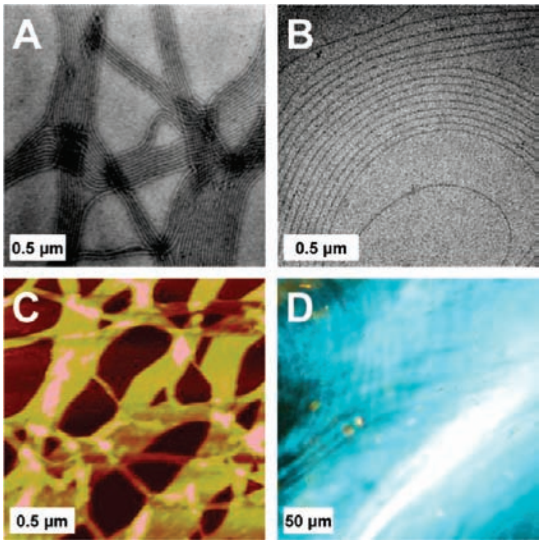

Figure 4. Nanofibers of **PEG45-AZO2**. Transmission electron micrograph obtained from a stained sample (A). Cryo-transmission electron micrograph of an unstained sample (B). AFM topography image (the vertical contrast is 20 nm) of a sample cast onto mica (C). Optical polarized micrograph of a 0.5 wt % aqueous solution of the nanofibers (D).

morphology of the self-assemblies obtained from these BCs (a point that will be discussed in the following section) and the presence of a metastable water dispersion of **PEG45-AZO16** prior to polymersome formation (see below). On completion of the turbidity measurements, the turbid mixtures were dialyzed against water to remove all dioxane. The morphology of the aggregates in the final water dispersions was then analyzed by UV−visible spectroscopy, TEM, cryo-TEM, and AFM.

3. Study of Polymeric Micellar Aggregates. In a first approach to study the aqueous self-assembly behavior of the **PEG*m*-AZO*n*** series, we investigated the UV−visible absorption spectra of the polymeric micellar self-assemblies dispersed in water and those corresponding to dioxane solutions of the BCs. As an example, the absorption spectra of the BCs **PEG45-AZO2** and **PEG45-AZO16** in dioxane solution are shown in Figure 3 along with the absorption spectra of the same BCs self-assembled in water (after dialysis). The absorption spectra of the BCs in dioxane show a maximum at around 360 nm, corresponding to the $\pi-\pi^*$ transition of isolated azobenzene molecules, together with a shoulder at longer wavelengths (around 450 nm) corresponding to the $n-\pi^*$ transition. A blue-shift and a broadening of the main absorption band is detected in the UV−vis spectrum of the polymeric self-assemblies obtained from **PEG45-AZO16** in water, and this is associated with the formation of dimers or higher number aggregates by π-stacking of azobenzene moieties in a parallel fashion (H-aggregation).[75] A similar feature is observed in the absorption spectra of the polymeric self-assemblies obtained from **PEG45-AZO4**, **PEG45-AZO8**, and **PEG114-AZO16** (see the Supporting Information). In contrast, the maximum of the absorption band of the polymeric self-assemblies from **PEG45-AZO2** is detected at around 365 nm (similar to that of **PEG45-AZO2** in dioxane solution) with two shoulders both at shorter and at longer wavelengths, indicating that H-aggregation does not take place to the same extent as in the polymeric self-assemblies obtained form **PEG45-AZO16**. The structure of the main absorption band of the self-assemblies of **PEG45-AZO2** in water apparently indicates more loosely packed azobenzene moieties similar to spherical micelles containing azobenzene surfactants.[88]

The morphology of the polymeric micellar self-assemblies was analyzed by TEM on samples stained with uranyl acetate, by cryo-TEM on native samples rapidly frozen in liquid ethane, or by AFM on samples cast onto mica (details on the preparation of the samples for TEM, cryo-TEM, and AFM are included in the Supporting Information). TEM images of stained samples of **PEG45-AZO2** (hydrophilic/hydrophobic ratio = 67/33) revealed bundles of nanofibers (Figure 4A) with dark regions corresponding to PEG domains and lighter areas corresponding to aromatic segments.[66] The individual nanofiber exhibited a uniform external diameter of 30 nm. Evidence for end units was not detected for these nanofibers so we can state that the length of the fibrils is higher than several micrometers (according to the accessible visible region in the TEM image with the lowest magnification). Similar nanofibers were detected by cryo-TEM (Figure 4B). By this technique, the diameter of individual nanofibers was measured to be 8 nm, which corresponds to the hydrophobic dendritic block of the BC. However, TEM with negative staining allowed the whole diameter of the nanofibers (30 nm) to be estimated, including the hydrophilic PEG and hydrophobic azodendron. The long cylindrical micellar mor-

---

(88) Kang, H.-C.; Min Lee, B.; Yoon, J.; Yoon, M. *J. Colloid Interface Sci.* **2000**, *231*, 255.

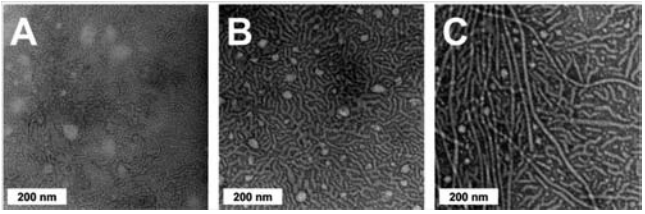

Figure 5. Transmission electron micrographs of the aggregates with 28 wt % (A), 36 wt % (B), and 50 wt % (C) of water added to the solutions of **PEG45-AZO2** in dioxane (initial concentration 1 wt %). (The irregular white spots in the three images are caused by staining artifacts.)

phology of the aggregates of **PEG45-AZO2** was also detected by AFM on samples cast onto mica (Figure 4C). Considering that the extended molecular length of the dendritic block (3.6 nm) is close to one-half the value of the diameter of core of the fiber, we consider that **PEG45-AZO2** self-assembles into cylindrical micelles consisting of a PEG corona and a core composed of azodendron blocks in which the cyanoazobenzene mesogenic units are approximately organized in a head-to-head manner.

As particles with a rod-like shape with a high aspect ratio can result in liquid-crystalline ordering,[89] the turbid dispersion of the cylindrical micelles of **PEG45-AZO2** in water was investigated by POM. A birefringent thread-like texture was observed for a sample with a concentration of 0.5 wt % (Figure 4D), indicating a lyotropic nematic phase.[66,90] As shown in the images obtained by TEM, cryo-TEM, or AFM, the long cylindrical micelles (nanofibers) generated in water show a marked tendency to align parallel to each other to form rigid bundles with a high aspect ratio. These bundles are likely to be responsible for the observed lyotropic behavior.

The aqueous aggregation of amphiphilic BCs to form nanofibers is an interesting subject due to the potential applications of fibrous micelles.[91] The availability of well-defined nanofiber-forming BCs is crucial in understanding the mechanisms of their self-assembly behavior. In this sense, we have investigated the evolution of **PEG45-AZO2** in dioxane on addition of water to generate the nanofibers described previously (Figure 4). It was mentioned above that the turbidity curve for this polymer shows three jumps before the final plateau is reached (Figure 2). We therefore studied the morphology of the intermediate aggregates corresponding with each turbidity plateau by TEM. Samples were prepared by applying a droplet of the dispersion (dioxane/water) directly onto the grid, followed by rapid blotting and staining using a dilute aqueous solution of uranyl acetate (this staining process served also as morphological quenching). The transmission electron micrographs of the aggregates with 28, 36, and 50 wt % of water added to the solutions of **PEG45-AZO2** in dioxane (initial concentration of BC 1 wt %) are shown in Figure 5. These TEM images clearly indicate that the self-assembly proceeded progressively from mainly short worm-like micelles at low water contents to longer cylindrical micelles at high water content. After dialysis (when water is the only solvent), very long nanofibers were finally obtained (Figure 4A). This process is driven by minimization of the interfacial energy. The addition of water increases the hydrophobic/hydrophilic interfacial energy, and, consequently, the system tends to minimize the interfacial area through a transition from small worm-like micelles to long cylindrical micelles.

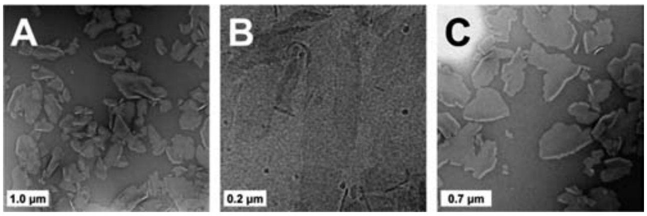

Figure 6. Transmission electron micrograph of the sheet-like aggregates formed in water by **PEG45-AZO4** (A). Cryo-transmission electron micrograph of the sheet-like aggregates of **PEG45-AZO4** (B). Transmission electron micrograph of the sheet-like aggregates formed in water by **PEG114-AZO16** (C).

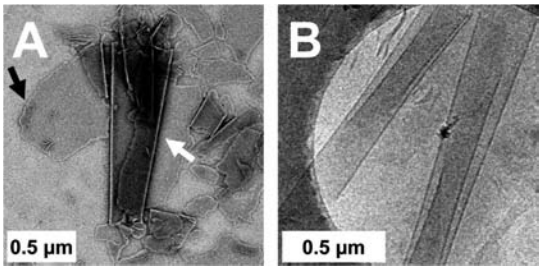

Figure 7. Transmission electron micrograph of the aggregates formed in water by the linear−dendritic BC **PEG45-AZO8** (A). The black arrow in (A) indicates a sheet-like aggregate. The white arrow in (A) indicates a tubular micelle. Cryo-transmission electron micrograph of the tubular micelles (B).

PEG45-AZO4, which has four cyanoazobenzene units at the periphery of the dendritic block and a hydrophilic/hydrophobic weight ratio of 50/50, self-assembled into sheet-like aggregates in water as revealed by TEM and cryo-TEM (Figure 6A and B, respectively). The thickness of the hydrophobic part of the sheets is of ∼7 nm (see the Supporting Information), which is also around twice the calculated length of fully extended azodendron block. Thus, we can propose a bilayer organization for the mesogen packing in the hydrophobic domains and a lamellar micelle structure with a PEG corona for the polymeric aggregates. The BC **PEG114-AZO16**, which has a lower hydrophilic/hydrophobic ratio (38/62) than **PEG45-AZO4**, a larger number of azobenzene units in the dendritic block ($n = 16$), and a higher degree of polymerization ($m = 114$) for the PEG chain, also formed sheet-like aggregates in water (Figure 6C).

A further decrease of the hydrophilic/hydrophobic ratio to 33/67 in the **PEG45-AZO*n*** series is obtained in **PEG45-AZO8**, which contains the generation 3 of azodendron. This BC formed sheet-like aggregates (see Figure 7A, black arrowhead) as well as tubular micelles (long curled sheet, white arrowhead in Figure 7A).[92] In cryo-TEM (Figure 7B), the structure of the tubular micelles is resolved into a gray core and two dark straight lines, which are the 2D projections of the tube cavity and the aromatic walls of the micelle, respectively.[93−95] The average diameter of the tubular micelles is about 150 nm, and the length can be roughly estimated to be between 0.5 and 2 μm. A membrane

---

(89) Yu, S. M.; Conticello, V. P.; Zhang, G.; Kayser, C.; Founier, M. J.; Mason, T. L.; Tirrell, D. A. *Nature* **1997**, *389*, 167.

(90) Ryu, J.-H.; Lee, M. *J. Am. Chem. Soc.* **2005**, *127*, 14170.

(91) Dreiss, C. A. *Soft Matter* **2007**, *3*, 956.

(92) Ambrosi, M.; Fratini, E.; Alfredsson, V.; Ninham, B. W.; Giorgi, R.; Lo Nostro, P.; Baglioni, P. *J. Am. Chem. Soc.* **2006**, *128*, 7209.

(93) Grbner, D.; Zhai, L.; Talmon, Y.; Schmidt, J.; Freiberger, N.; Glatter, O.; Herzog, B.; Hoffmann, H. *J. Phys. Chem. B* **2008**, *112*, 2901.

(94) Yang, W.-Y.; Lee, E.; Lee, M. *J. Am. Chem. Soc.* **2006**, *128*, 3484.

(95) Liu, Q.; Wang, Y.; Li, W.; Wu, L. *Polymer* **2008**, *49*, 4159.

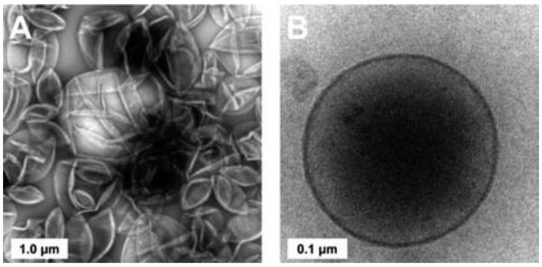

Figure 8. Transmission electron micrograph of the polymersomes formed in water by the linear−dendritic BC **PEG45-AZO16** (A). Cryo-transmission electron micrograph of the polymersomes (B).

thickness of about 7 nm was measured for both sheet-like and tubular micelles according to the cryo-TEM images, indicating a bilayer organization.

The generation number 4 of azodendron in BC **PEG45-AZO16** gives rise to an even lower hydrophilic/hydrophobic weight ratio of 20/80. This linear−dendritic BC formed vesicles, that is, closed sheet-like micelles, which appear as deflated vesicles by TEM because of sample drying, as shown in Figure 8A. The undisturbed shape of the vesicles was apparent by cryo-TEM (Figure 8B). The diameter of the vesicles, as measured from the cryo-TEM images, typically ranges from 300 to 800 nm. The thickness of the membrane was found to be 10 nm, which is twice the length of the dendritic block. This feature indicates that the membrane of the vesicles has a bilayer structure in a way similar to that of the sheet-like aggregates obtained from **PEG45-AZO4**, **PEG45-AZO8**, and **PEG114-AZO16**. A similar result has already been described for polymersomes based on amphiphilic linear−linear LC BCs.[72]

In summary, the formation of polymeric self-assemblies in water was observed for the linear−dendritic BCs **PEG*m*-AZO*n*** with hydrophilic/hydrophobic ratios ranging from 67/33 to 20/80 (macroscopic phase separation was detected in the case of **PEG25-AZO16**, with a hydrophilic/hydrophobic ratio of 12/88). A generation-dependent aggregation behavior from cylindrical micelles to vesicles has been demonstrated for the **PEG45-AZO*n*** ($n = 2, 4, 8, 16$) series. A schematic representation of the self-assembly and packing of **PEG45-AZO2** and **PEG45-AZO16** is given in Figure 9. As the size of the hydrophobic dendritic block increases, the morphological transition of the polymeric aggregates from cylindrical micelles (nanofibers) to sheet-like micelles and eventually to vesicles is driven by the minimization of the interfacial energy and qualitatively follows the theory of Israelachvili et al.[96,97] The packing parameter $p = v/al$ of **PEG45-AZO2** in aqueous solution (with the generation 2 of azodendron and a hydrophilic/hydrophobic weight ratio of 67/33) should be around 1/2 for cylindrical micelle formation (where v is the hydrophobic volume, a is the optimal interfacial area, and l is the length of the hydrophobic block normal to the interface). As the generation number, that is, the volume of the hydrophobic block, increases with the same PEG block, the value of p increases and approaches 1. As a consequence, parallel molecular packing and a bilayer structure become more stable. In the case of **PEG45-AZO4** (hydrophilic/hydrophobic wt ratio of 50/50) and **PEG45-AZO8** (hydrophilic/hydrophobic wt ratio of 33/67), sheet-like micelles are observed. In **PEG45-AZO8**, the sheet-like aggregates become so large and the energy cost due to surface tension effects becomes so great, that some sheets curl to form tubular micelles. In the case of **PEG45-AZO16** (hydrophilic/hydrophobic wt ratio of 20/80), all sheets curl in all directions and literally become closed on forming vesicles to minimize the surface tension effects. The observation of a tubular morphology together with sheet-like aggregates in **PEG45-AZO8** may indicate that the tubular aggregates are stable intermediates between sheet-like micelles and vesicles.[98] The first contribution in the field of linear−dendritic BCs also described an Israelachvili-type assembly behavior as a function of the generation number of the dendritic block.[56] In this early example, the hydrophobic block was a fixed-length linear polystyrene (PS), while the hydrophilic block was based on a series of dendrons with different sizes. In the **PEG45-AZO*n*** series, the hydrophobic block is based on the first four generations of hydrophobic azodendrons, while the hydrophilic block is a fixed-length linear PEG. Therefore, consideration of the packing parameter can be used qualitatively and generally in the prediction of the self-assembly of amphiphilic linear−dendritic BCs.

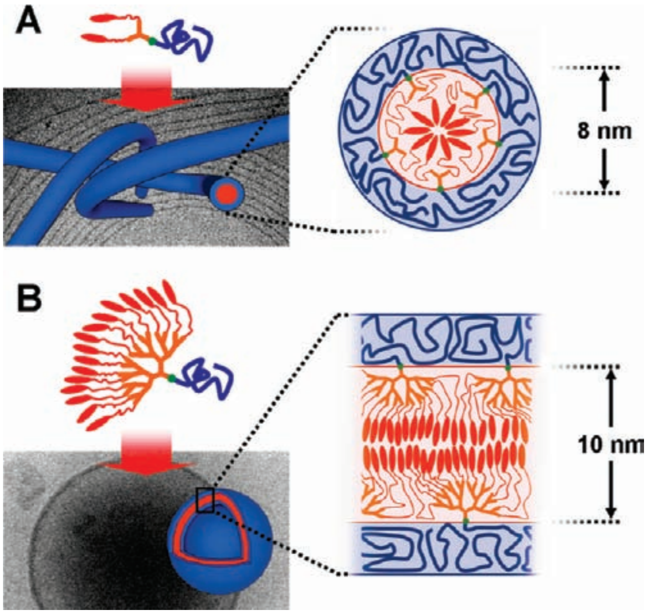

Figure 9. Schematic representations of the chain structures and the polymeric self-assemblies of **PEG45-AZO2** (A) and **PEG45-AZO16** (B) in water together with the proposed models for the packing of the BCs in the polymeric self-assemblies. In the cartoons, the PEG corona is in blue, the dendron arms in the hydrophobic core are in orange, and azo-mesogens are in red.

Besides the consideration of interfacial energy, other driving forces such as $\pi-\pi$ stacking and/or dipole interactions between the aromatic segments and additional liquid crystalline interactions in the hydrophobic part may favor parallel molecular packing in sheet-like micelles and vesicles.[72,96,99−101] The branched architecture of the hydrophobic block with mesogens at the periphery also favors their packing and the formation of self-assemblies. Indeed, H-aggregation of azobenzene moieties

---

(96) Israelachvili, J. N.; Mitchell, D. J.; Ninham, B. W. *J. Chem. Soc., Faraday Trans. T.2* **1976**, *72*, 1525.
(97) Antonietti, M.; Förster, S. *Adv. Mater.* **2003**, *15*, 1323.
(98) Eisenberg, A.; Yu, K. *Macromolecules* **1998**, *31*, 3509.
(99) Song, B.; Wei, H.; Wang, Z.; Zhang, X.; Smet, M.; Dehaen, W. *Adv. Mater.* **2007**, *19*, 416.
(100) Jia, L.; Cao, A.; Lévy, D.; Xu, B.; Albouy, P.-A.; Xing, X.; Bowick, M.; Li, M.-H. *Soft Matter* **2009**, *5*, 3446.
(101) Xu, B.; Piñol, R.; Nono-Djamen, M.; Pensec, S.; Keller, P.; Albouy, P.-A.; Lévy, D.; Li, M.-H. *Faraday Discuss.* **2009**, *143*, 235.

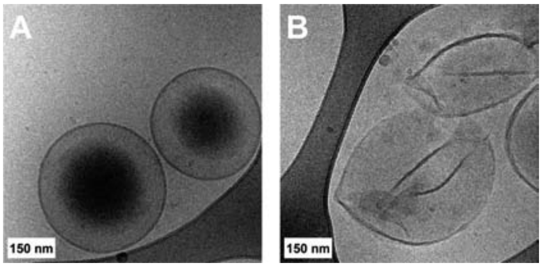

Figure 10. Cryo-transmission electron micrograph of the polymersomes formed in water by the linear−dendritic BC **PEG45-AZO16** before (A) and after illumination with 360 nm unpolarized light (150 mW/cm^2) for 35 min (B).

in our polymeric self-assemblies (detected by UV−vis spectroscopy (Figure 3)) was higher in the polymersome dispersion of **PEG45-AZO16** than in the cylindrical micelle dispersion of **PEG45-AZO2**.

Self-assembly of BCs by slow and progressive addition of water into a polymeric solution, as it has been described in this Article, is a widely used method for preparing well-defined micellar structures. However, direct self-assembly in water is preferred for practical purposes. To check the direct formation of micelles, we tried to disperse some of the BCs (**PEG45-AZO4** and **PEG114-AZO16** were selected as examples) by applying a sonication probe in a mixture of water and polymer (0.5 wt % of block copolymer). Preliminary results indicate that self-assembly does take place. Nevertheless, the polymers are only partially dispersed in water, and most of the polymeric sample remains insoluble (see the Supporting Information).

4. UV Illumination of the Aqueous Polymersome Dispersion. Polymersome is a very interesting type of polymer self-assembly because it can be used as a carrier for hydrophilic substances (in the interior compartment) as well as hydrophobic substances (in the membrane) for applications in the fields of drug delivery, medical imaging, or material chemistry.[2] A crucial question is how to release the encapsulated active substances when and where they are needed. The azobenzene-containing linear−dendritic polymersomes reported here can be considered as a model system for photoresponsive polymersomes. To test this idea, an illumination experiment was carried out on the polymersome dispersion in water. The typical cryo-TEM images of the polymersomes before and after UV illumination are shown in Figure 10A and B, respectively. After illumination, the vesicle membrane was distorted, and wrinkles, even rupture, are clearly visible in Figure 10B. The azobenzene groups in the middle of the membrane undergo a trans-to-cis isomerization during UV exposure, and this may result in a change of the membrane structure. This feature could be responsible for the morphological changes in polymersomes (Figure 10B). Similar phenomena were observed by optical microscopy in the giant symmetrical polymersomes made from linear−linear azobenzene-containing BC.[83] This preliminary study demonstrates that the polymersomes made from azobenzene-containing linear−dendritic BC are photoresponsive. Detailed investigations into the photoresponsive properties of polymersomes for model substance release are in progress.

Conclusions

The aqueous self-assembly behavior of a new class of amphiphilic linear−dendritic BCs is reported. These materials are composed of PEG as the hydrophilic block and the first four generations of azobenzene-containing dendrons based on 2,2-bis(hydroxymethyl)propionic acid (bis-MPA) as the hydrophobic block. The hydrophilic/hydrophobic ratio of these BCs was varied by changing the generation number of the dendritic block or the length of the PEG block. Polymeric micellar aggregates were observed for hydrophilic/hydrophobic ratios ranging from 67/33 to 20/80. A morphological transition of the polymeric aggregates in water from cylindrical micelles (nanofibers) to sheet-like micelles and eventually to vesicles has been demonstrated for the **PEG45-AZO*n*** series ($n = 2, 4, 8, 16$) by increasing the generation number of the hydrophobic dendritic block. Tubular micelles, which might be intermediates in the sheet-like aggregate-to-polymersome transition, have been identified for **PEG45-AZO8**. The primary driving force responsible for the aggregation behavior is the minimization of the interfacial energy governed by the balance between the hydrophilic interaction of the linear PEG and the hydrophobic interaction of the azodendron block. However, other driving forces such as $\pi-\pi$ stacking, dipole interactions, liquid-crystalline ordering, and the preorganized branched architecture of the dendritic block should also be considered. A UV illumination study clearly showed that the polymersomes made from **PEG45-AZO16** are photoresponsive. These polymersomes may find interesting applications where stimuli-responsive properties are required.

Acknowledgment. This work was supported by the MICINN, Spain, under the project MAT2008-06522-C02, FEDER, and DGA fundings. J.d.B. acknowledges a grant from DGA and CAI. We also acknowledge Daniel Lévy of the PICT-IBISA Imaging Facility in the Institut Curie, Mª Ángeles Laguna of the Servicio de Microscopía Electrónica-Universidad de Zaragoza, and Emma Rossinyol of the Servei de Microscòpia-Universitat Autònoma de Barcelona, for the TEM and cryo-TEM observations, and Jordi Díaz of the Serveis Cientificotècnics-Universidad de Barcelona for AFM measurements. We thank E. Mabrouk for his help in the illumination experiments of polymersomes. M.-H.L. thanks Ming Jiang for cooperation supported by the senior visiting scholar foundation of the key laboratory at Fudan University.

Supporting Information Available: Materials and techniques. Chemical structures of the **PEG*m*-AZO*n*** linear−dendritic BCs. Details of the synthesis and characterization of **PEG25-AZO16** and **PEG114-AZO16** and the corresponding MALDI-TOF mass spectra and DSC traces. Details of the preparation and morphological characterization of polymeric micellar aggregates. Procedure for the UV illumination of the aqueous polymersome dispersion. This material is available free of charge via the Internet at http://pubs.acs.org.

JA9083946